Journal of Composites for Construction, Vol. 7, No. 2, May 2003, pp.154-163

BOND BETWEEN CFRP BARS AND CONCRETE: PART I – EXPERIMENTAL STUDY

L. J. Malvar[1], J.V. Cox[2], and K. Bergeron Cochran[3]

The bond characteristics of four different types of carbon fiber reinforced polymer (CFRP) rebars (or tendons) with different surface deformations embedded in lightweight concrete were analyzed experimentally. In a first series of tests, local bond stress-slip data, as well as bond stress-radial deformation data, needed for interface modeling of the bond mechanics, were obtained for varying levels of confining pressure. In addition to bond stress and slip, radial stress and radial deformation were considered fundamental variables needed to provide for configuration-independent relationships. Each test specimen consisted of a CFRP rebar embedded in a 76-mm (3-inch) diameter, 102-mm (4-inch) long, precracked lightweight concrete cylinder subjected to a constant level of pressure on the outer surface. Only 76 mm (3 inches) of contact were allowed between the rebar and the concrete. For each rebar type, bond stress-slip and bond stress-radial deformation relationships were obtained for four levels of confining axisymmetric radial pressure. It was found that small surface indentations were sufficient to yield bond strengths comparable to that of steel bars. It was also shown that radial pressure is an important parameter that can increase the bond strength almost threefold for the range studied. In a second series of tests, the rebars were pulled out from 152-mm (6-inch) diameter, 610-mm (24-inch) long lightweight concrete specimens. These tests were conduced to provide preliminary data for development length assessment and model validation (Part II).

Keywords: bond (concrete to reinforcement); fiber reinforced polymer; FRP; concrete; composites; carbon; rebar; confinement; development length.

INTRODUCTION

Extensive and costly condition assessment, repair, and rehabilitation programs are under way to extend the service life of reinforced concrete structures. The main cause of deterioration is the corrosion of the steel reinforcement exposed to marine environment and aggressive agents such as deicing salts for bridges and pavements. To prevent this deterioration, fiber reinforced polymer (FRP) bars have recently been used, which have good corrosion resistance and some mechanical properties similar to steel. FRP rebars, tendons and grating have already been used in waterfront structures and bridges (Benmokrane and Rahman 1998; Dolan et al. 1999; Razaqpur 2000; Saadatmanesh and Ehsani 1998).

[1] Research Materials Engineer, Naval Facilities Engineering Service Center, Port Hueneme, CA 93043
[2] Visiting Researcher, Army Research Laboratory, APG MD 21005
[3] Graduate Student, Civil Engineering Department, University of Illinois at Urbana-Champaign, IL 61801

Two drawbacks with Aramid FRP (AFRP) and Glass FRP (GFRP) bars are their durability problems in alkaline, ultraviolet, and moist environments, as well as their low creep rupture strength (Malvar 1998; Yamaguchi et al. 1997), which are reflected in the current codes (ACI 440 2001; Bakht et al. 2000; Sonobe et al. 1997). Hence the current study only considered 4 types of CFRP bars, which can be used as reinforcements or prestressing strands.

The U.S. Navy is currently applying FRP materials to upgrade its waterfront reinforced concrete structures, and is considering their application as reinforcing or prestressing bars in lightweight concrete floating structures. There is, however, little knowledge on the mechanical interaction, i.e. bond, between these bars and lightweight concrete. This study focuses on the bond behavior of 4 carbon FRP (CFRP) bars within lightweight concrete (Figure 1 and Table 1). For each FRP rebar type, tensile tests are first carried out, then bond stress-slip responses under constant radial confining stress are experimentally determined, and finally pull-out tests for large embedment length specimens are completed. In the work presented in Part II, the data presented here is used to calibrate an interface bond model that, combined with various specimen models, is then used to provide preliminary design data for one of the bars.

RESEARCH SIGNIFICANCE

The acceptance of FRP rebar in structural engineering had been inhibited partly due to the lack of design criteria, particularly with regard to bond. While recent codes now address bond (ACI 440 2001; Bakht et al. 2000; Sonobe et al. 1997), little experimental data is available for bond in lightweight concrete, and even less for CFRP bars in lightweight concrete. The variation in bar deformation geometry and composition results in highly variable bond characteristics. Comparison of bond properties of various types of deformations is a first step in the determination of optimum deformation geometry.

The determination of more general bond stress-slip models is useful for mathematical or numerical modeling of reinforced concrete structural behavior. In particular, these models can be used to estimate anchorage requirements for reinforcing bars without the need for extensive testing. Anchorage requirements can also be verified via long embedment tests capable of developing the bars.

IMPORTANCE OF LATERAL CONFINEMENT

In spite of its importance, only a limited amount of research has included radial normal stress and deformation directly in the model (Cox and Herrmann 1992, 1998, 1999; Cox 1994, 1998; Cox and Guo 1999; Cox et al. 2000; Gambarova et al. 1998; Malvar 1992a, 1992b, 1992c, 1995; McCabe and Pantazopoulou 1998; Tork 1999; Lundgren 2000; FIB 2000). In many cases, a specimen configuration is chosen and no attempt is made at evaluating the confinement provided by the reinforced or unreinforced concrete surrounding the bar. A simple pull-out test with or without preset passive confining reinforcement (e.g. Sonobe et al., 1997) is often assumed to be representative of any actual confinement. As a result, very disparate configuration-dependent relationships for bond stress versus slip have been obtained, with variations in bond stress over 100 percent, e.g. Figure 3.16 from ASCE (1982), or Figure 6 from Keuser and Melhorn (1987). However, if the lateral confinement is included in the model, various experimental results can be reproduced with acceptable accuracy (Cox and Guo 1999;

Cox and Hermann 1992; FIB 2000). Recent state-of-the-art reports on bond of FRP bars by Taly and GangaRao (2001) and Tepfers et al. (Chapter 7 of FIB, 2000) also discuss confinement effects.

PREVIOUS WORK ON BOND OF FRP REBARS

Cosenza et al. (1999) studied the development length of a GFRP rebar similar to Type A used here (Figure 1). They found a bond strength of 14.5 MPa (2100 psi) at a slip of 0.25 mm (0.01 inch). They reported an embedment length of about $10d_b$ (bar diameters) for a #4 bar (Table 2). The same GFRP Type A rebar was used by Shield et al. (1999), who reported a development length of about $20d_b$ to $24d_b$ (the latter was used), with an equivalent bond strength of 5.4 to 4.5 MPa (780 to 650 psi), for a #5 bar (Table 2). The difference in development length could be due differences in bar size and concrete strengths (Table 2). ACI 440 (2001) indicates that the development length ℓ_{bf} can be expressed as a function of bar diameter d_b (or cross sectional area), concrete strength f_c', and bar design tensile strength f_{fu} (considering reductions for service environment) as:

$$\ell_{bf} = K_2 \frac{d_b^2 f_{fu}}{\sqrt{f_c'}} \qquad (1)$$

where K_2 is a constant for a particular bar. Alternatively, since the concrete strength effect is low, and assuming that the dependency on bar diameter is linear, ACI 440 (2001) also provides the following conservative design estimate:

$$\ell_{bf} = d_b f_{fu} / 2700 \text{ (in psi units)} \quad \text{or} \quad \ell_{bf} = d_b f_{fu} / 18.5 \text{ (in SI units)} \qquad (2)$$

On the low end, a 70 ksi GFRP bar in an aggressive environment would result in $\ell_{bf} = 18\ d_b$, while a 170 ksi CFRP bar would result in $\ell_{bf} = 56\ d_b$. The Japanese code recommends $23d_b$ (Sonobe et al. 1997).

Various authors have also worked on the bond of the Type D bar (Benmokrane and Chennouf 1997; Cox and Guo 1999; Mahmoud et al. 1999; Tepfers et al. 1992; Tokyo 1989) (see Table 2).

TENSILE AND BOND TESTS FOR CFRP REBARS

Rebar Types

Four types of CFRP rebars (or tendons) with different deformations were considered (Figure 1). For each one, Table 1 reports the deformation spacing (or length of surface structure pattern) and height. The deformation height is measured as the difference between the bar radius at a deformation and the radius at midpoint between that deformation and the next one. In addition each rebar type presents the following characteristics:

- Type A bars have molded external deformations that mimic those of steel rebar. An outer layer consisting exclusively of matrix material is provided around the fibers for

additional protection. The deformation height was about 0.6 mm (0.024 in) and the spacing was 7.6 mm (0.3 in) (Table 1).

- The surface of Type B bars was roughened to obtain very small deformations (0.0025 mm or 0.001 in high) very closely spaced (3.0 mm or 0.12 in).
- Type C bars are actually tendons fabricated by twisting and gluing 7 separate CFRP smooth strands. Although originally developed for prestressing applications, these tendons can be used as reinforcing bars. The twist on the strands was low, resulting in an equivalent deformation spacing in excess of 150 mm (6 in) (Table 1).
- Type D bars are also 7 strand tendons (see Table 1 for properties).

Tensile Tests

Tensile tests similar to ASTM D 3916 (1984) were first conducted on each type to verify the ultimate strength and longitudinal elastic modulus. First a single test was completed per bar, where the samples were 1.83 m (6 feet) long, with the ends epoxied into 0.61 m (2 feet) long steel pipes prior to placing them in the grips. Measured values are reported in Table 1. For bar Types C and D, these values matched the minimum expected values, e.g. see Iyer at al. (1994) for Type C, and Tokyo Rope (1989) for Type D (see Table 2). For Type A, two more tests were completed, which resulted in a coefficient of variation of only 1.5% (see Table 1).

Bond Tests

The objective of these tests was to determine configuration-independent, local bond stress-slip data for development and calibration of more general bond models (i.e., models that incorporate the normal component of the interface traction and the radial deformation). Typically bond stress-slip relations are derived from pull-out tests, or other more complex setups, without regard for the lateral confinement exerted by the particular setup. As a result very disparate behaviors have been obtained which are dependent on the particular setup. The current setup uses a very small specimen in an attempt to identify local data experimentally (an alternative is to use an analytical or numerical model that relates local response to measured global responses – an inverse method, e.g. Focacci et al., 2000). If the lateral confinement on this specimen is systematically varied between tests, a family of curves can be obtained, which can potentially be used to derive a bond model that is configuration independent. Similar tests have already been carried out for steel and GFRP bars (Malvar 1992a, 1992b, 1992c, 1995) yielding general bond-slip relationships that were successfully used in predicting a variety of well known results (Cox 1994; Cox and Guo 1999; Cox and Herrmann 1992, 1998, 1999). For FRP bars, the bond strength is more affected by the low transverse stiffness (which is mostly dependent on the matrix material).

The specimen used is shown in Figures 2, 3 and 4. It consists of a 76-mm (3-inch) diameter, 102-mm (4-in) long concrete cylinder surrounding an FRP bar. Only about 76 mm (3 in) of the bar were actually in contact with the concrete, contact being prevented in the rest of the specimen via silicone-rubber spacers. The outer concrete surface was surrounded by a split, threaded steel pipe that carried the pullout force via shear stresses in the threaded region (Figures 2, 3). The pipe was split into 8 strips in order to essentially eliminate its lateral resistance. The concrete cylinder was actually cast in place against the pipe threads (Figure 4). Casting was carried out with the specimen placed vertically. As shown in Figure 2, on the unloaded side

(inside the pipe) the bar extended beyond the concrete specimen, so that new, undisturbed bar was pulled into the bond zone as the test progressed, maintaining the same contact length.

The radial confining pressure on the specimen was applied via a thin ring that surrounds the portion of pipe containing the concrete cylinder. A thin coat of bearing grease prevented any friction between the ring and the pipe. A hydraulic jack with an adjustable relief valve closed the ring with a constant force during the test. In this way the longitudinal reaction and the radial confinement could be both controlled and measured independently of each other.

Concrete mix proportions were:

- Type II cement 406 Kg/m^3 (685 lbs/yard^3)
- Class F fly ash 82 Kg/m^3 (138 lbs/yard^3)
- Water 205 Kg/m^3 (345 lbs/yard^3)
- Expanded shale coarse aggregate 449 Kg/m^3 (756 lbs/yard^3)
- Expanded shale fine aggregate 648 Kg/m^3 (1092 lbs/yard^3)

In addition, air entrainment was used to obtain 6% to 8% air, and a plasticizer was used to obtain a 4" slump. Three uniaxial unconfined compressive tests and three tensile splitting tests were completed on 76-mm by 152-mm (3-in by 6-in) cylindrical specimens at 28 days. Concrete properties are reported in Table 3.

On the loaded end, two linear variable differential transformers (LVDTs) were clamped to the bar and measured the relative displacement of the outer concrete surface, i.e. the pipe. They were diametrically opposed to compensate for any rotation. A third LVDT was located inside the pipe and measured the relative displacement (slip) between the pipe and the unloaded end of the bar. Finally a fourth LVDT measured the opening of the confining ring. This was later translated into a radial deformation or dilation. The apparatus was installed in an MTS testing machine. The MTS load cell provided pullout load measurements. Average bond stresses were calculated by dividing pullout loads by the contact area between the bar and concrete.

Prior to each bond test, the concrete cylinder was precracked by loading the split pipe laterally as in a Brazilian test. Upon crack initiation, the specimen was then placed in the MTS testing machine, a confining pressure at the bar surface was set at either 3.45, 10.3, 17.2, or 24.1 MPa (500, 1500, 2500, or 3500 psi) and kept constant during the remainder of the test. After the precracking, and assuming that the cracks are open, all the pressure from the confining ring is transferred to the bar. All tests were carried out under longitudinal displacement control.

Long Embedment Tests

In these tests, the CFRP rebars were pulled out from 152-mm (6-in) diameter, 610-mm (24-in) long lightweight concrete specimens (Figure 5). The U.S. Navy requires covers over reinforcement between 65 and 75 mm (2.5 and 3 in) for marine concrete, the latter for concrete in the splash zone (Unified 1999), and this specimen provides a similar cover. These specimens also provided additional data for the estimation of development lengths in Part II of this paper. The test set up and a tested specimen are shown in Figure 6. The first 76 mm (3 in) of the rebars embedded in the cylinders were prevented from bonding to the concrete, hence the embedded length is only 534 mm (21 in). Two test specimens were tested per bar type. Load and free end displacement were measured.

Concrete properties for the long embedment tests are indicated in Table 3. Note that this is lightweight concrete, which typically has a low modulus of elasticity compared to normal weight concrete.

EXPERIMENTAL RESULTS

Bond Tests Results: Complete Bond Stress-Slip Curves

Four curves are reported for each bar type, correspond to confining pressures at the bar surface of 3.45 through 24.1 MPa (500 through 3500 psi) in 6.9 MPa (1000 psi) increments, as mentioned earlier. Each curve is typically the average of 2 or 3 tests. The slip mentioned in this section is the average measurement of the two LVDTs located on the loaded end of the bar. This measurement was corrected for the unbonded length of rebar and the gage offset. Figure 4 shows the cracks that formed for Type B (test at confining stress of 17.2 MPa or 2500 psi). Figures 7 through 10 show the complete bond stress versus loaded-end slip response for all 4 bars and all 4 confining pressures. Table 4 shows the peak bond stresses and corresponding slips.

1) Type A. Figure 7 reports the bond stress versus slip behavior for Type A bars, up to a displacement of 8 mm (0.315 in). Near 7.6 mm (0.3 in) of slip, the bond stress start to increase again, indicating that the bar has advanced one deformation spacing. The bond stress can be increased 2.5 times to about 10 MPa (1450 psi) by varying the confining pressure from 3.45 to 24.1 MPa (500 to 3500 psi). The deformations in this bar were able to sustain the very high bond stresses: after displacing about 3 deformation spacings the deformations could still provide significant bond strengths. Previous research (Achillides et al. 1997) indicates that for low concrete strengths (15 to 30 MPa) the concrete is crushed between the ribs (and the bond strength is dependent on the concrete strength). For higher concrete strengths, the CFRP ribs are damaged instead (and the bond strength is no longer affected by the concrete strength). For 19-mm (3/4-in) diameter plain steel bars, bond stresses around 19.3 MPa (2800 psi) were obtained for the highest confining pressure used here (Malvar 1992a, 1992b, 1992c). For 19-mm (3/4-in) diameter GFRP bars, bond stresses around 11.7 MPa (1700 psi) were obtained for the highest confining pressure used here (Malvar 1995). The latter GFRP bars had deformation heights of at least 5.4% of the diameter, compared with 6% for the current Type A CFRP bar.

2) Type B. The deformations in these bars had a height of only 0.3% of the nominal diameter, and were not sufficient to induce significant lateral displacement. As a result, confining stresses above 3.45 MPa (500 psi) appeared to prevent the longitudinal cracks from opening, and thus no increase in bond stress can be observed for the higher confining pressures (Figure 8) (the variation in bond strength is attributed to experimental scatter). A “squeeze-through” failure mode was apparent (see Chapter 7 of FIB, 2000), with maximum bond stresses around 4 MPa (580 psi). After about every 3 mm (0.12 in) of displacement, the bond stresses increase again, indicating that the bar displaced one deformation length (Figure 8).

3) Type C. These bars tended to twist as they were being pulled out, since the test arrangement does not constrain the twisting motion. Because the deformation spacing is very large (about 15 times the diameter, see Table 1), the bars tend to slowly “unscrew from the concrete” producing

very small lateral displacements, and resulting in small bond stress increases with increasing confining pressure (Figure 9), and bond strengths below 6 MPa (870 psi). The bond stress remained somewhat constant towards the end of the tests, which may allow for redistribution of stresses in the structural member. However, due in part to the twisting, the demonstrated bond behavior may not be representative of the bond response of a bar bridging a primary crack.

4) Type D. These bars have significant deformations, and the bond stress could be almost doubled by increasing the confining pressure (Figure 10). The maximum bond stresses measured were almost as high as for Type A. Also, the relatively large deformation spacing allowed for significant displacement at almost constant bond stress. This plastic behavior is advantageous because it may allow for redistribution of forces in the structure (and overall higher load-carrying capacity) without failure.

5) Bar Deformations. From these limited tests, and previous ones on GFRP bars (Malvar 1995), some very preliminary conclusions could be drawn to avoid "squeeze-through" failures and low bond strengths: (a) deformation heights of about 6% of the diameter, or more, may be necessary, (b) deformation spacings of 3 times the diameter, or less, may be necessary.

Bond Tests Results: Bond Stress-Radial Displacement Curves

Upon first loading, the rebar deformations exert radial pressures against the surrounding concrete potentially splitting the concrete longitudinally, or, if precracked, until the longitudinal cracks start opening. If external confinement is provided, the rebar tends to slowly open the concrete cracks until enough space is created for the deformations to advance, via a combination of sliding, concrete crushing, and damage to the bar deformations (or surface structure). Eventually, after enough combined damage has taken place, a radial contraction may occur (Malvar 1992a, 1992b, 1992c, 1995). To capture this dilation/contraction the ring opening was measured, which is converted to a radial displacement at the outer surface of the concrete cylinder specimen. The bond stress versus radial displacement curves obtained are shown in Figures 11 and 12. For each rebar type the following was observed:

1) Type A. A response qualitatively similar to that of steel (or some GFRP) rebars was obtained. Figure 11 shows the results after a displacement in excess of 2 deformations spacings. While advancing one deformation length, the curve presents 4 behavior regimes, as follows:

- First the load increases without much radial opening, indicating that the bar cannot advance much due to interlocking between each deformation and the surrounding concrete.
- Second the generated radial pressure caused by the wedging action of the ribs is high enough that the concrete cracks open quickly, enough to allow for each deformation to advance (high radial dilation at almost constant bond stress).
- Third, slip increases while the radial opening remains constant, and the load decreases.
- Fourth, once the bar has advanced one deformation length (i.e. one deformation has taken the place of the previous one), the concrete cylinder quickly contracts radially at fairly constant load.

These four behavior regimes produce somewhat of a rectangular curve in the bond stress versus radial dilation plot (see Figure 11 for lower two confining pressures). If the bar advances one more deformation length, another rectangular curve (cycle) is obtained within the previous one, and so on. Figure 11 shows about 2.5 cycles, indicating a total slip of about 2.5 deformation spacings. The drop in maximum bond stress after each cycle is also apparent. For high lateral confinement, the rectangular shape contracts, indicating that, after displacing one deformation length, the deformations themselves and the concrete around them are damaged enough to prevent any significant further radial dilation (Figure 11, higher two confining pressures). Measurement of the deformations after test completion indicated they had retained about 86% of their original height if tested under 3.45 MPa (500 psi) confinement, 82% if tested under 10.3 MPa (1500 psi) confinement, 45% under 17.2 MPa (2500 psi) confinement, and 37% under 24.1 MPa (3500 psi) confinement.

2) Type B. The deformations' height (0.3% of the diameter) was not sufficient to induce significant radial dilation. The measurement was as small as the instrumentation noise, and the data are not reported.

3) Type C. The deformations' spacing was too large to induce significant radial dilation. The observed twist could also reduce the dilation. The measured radial dilation would not show on a graph with the same scale as Type A.

4) Type D. Significant dilation is observed, which is reported in Figure 12. Since the displacement never reached one deformation length, no contraction is observed.

Long Embedment Tests Results

Depending on the bar type, the embedment length and confinement provided by the long concrete cylinder were in some cases sufficient to develop the bar. If the bar did not break, failure was obtained by vertical splitting of the concrete cylinder, typically into three approximately 120° longitudinal segments (Figure 13). These tests results are shown in Table 5.

1) Type A. The developed bar stress at cylinder splitting reached up to 79% of ultimate (Table 5). From Part II of this paper, in this setup the development length is estimated to be 357 mm (14 in) or 35 d_b, if the concrete cover had been sufficient to not split. This would yield $K_2 = 1/37$ in equation (1) – in psi units to compare with ACI 440 (2001). This supports that equation (2) is conservative since it would predict 84 d_b for normal weight concrete, and 109 d_b if a factor of 1.3 is used to account for lightweight concrete (ACI 318, 1999). Note also that in actual applications the presence of stirrups provide additional lateral confinement that would reduce both the development length and the required cover.

2) Type B. One bar broke, i.e. was developed with 533 mm (21 in), but the other only reached 1248 MPa (181 ksi). As a local approximation for this second bar, assuming that strength and development length are locally linearly related as in equation (1), in this setup the development length could be as high as 622 mm (24.5 in) or 76 d_b to develop the expected tensile strength from the tensile tests (Table 1). This would yield $K_2 = 1/10.4$ in equation (1) – in psi units to compare with ACI 440 (2001). This can also be compared with a conservative 78 d_b from

equation (2) for normal weight concrete (and 101 d_b if a factor of 1.3 is used to account for lightweight concrete).

3) Type C. The strands in this bar are relatively smooth, and show very little twist around the longitudinal axis. Using the average stress in the bar at concrete splitting (from Table 5) as hypothetical f_{fu}, equation (2) would have estimated a development length around 76 mm (30 inches). This appears to support that equation (2) is conservative.

4) Type D. In the second test, the cylinder split near the rebar strength, so the development length in this setup would be around 562 mm (22 in) or 57 d_b. This would yield K_2 = 1/25.8 in equation (1) – in psi units to compare with ACI 440 (2001). This can also be compared with a conservative 100 d_b from equation (2) for normal weight concrete (about 130 d_b for lightweight).

ANALYTICAL MONOTONIC ENVELOPE

Analytical expressions for the monotonic bond stress-slip response are commonly used in simplified models for bond. Most structural problems will need modeling below ultimate (e.g. at the service state level), so it was decided to fit a model only to the ascending branch of the bond stress versus slip response (the post-peak response is also gage-length dependent and more difficult to use). This expression is derived in a two step procedure. First the peak on the bond stress-slip curve is defined as a function of confinement as follows:

$$\tau_m / f_t = A + B\, \sigma / f_t \tag{3}$$

$$s_m / \varnothing = C + D\, \sigma / f_t \tag{4}$$

where

τ_m = bond strength (peak bond stress)
σ = confining axisymmetric radial pressure
f_t = tensile strength
s_m = slip at peak bond stress
$\varnothing$ = nominal bar diameter
A, B, C, D = non-dimensional empirical constants for each bar type (Table 6).

Second, the ascending normalized bond stress-slip curve can be expressed using the model by Ciampi et al. (1981), also known as the BEP model (Eligehausen et al. 1983; Cosenza et al. 1995, 1997):

$$\tau = \tau_m (s/s_m)^{\alpha} \tag{5}$$

or using the CMR model (Cosenza et al. 1995, 1997):

$$\tau = \tau_m (1-\exp\{-s/s_r\})^{\alpha} \tag{6}$$

where α and s_r are empirical constants for each bar type. The CMR model has 2 parameters, so it is capable of better approximation within the range $0 \le \tau \le \tau_m$. Since s_r has a unit of length, it was replaced by $s_r = s_m / \beta$, where β is a non-dimensional parameter. Hence a modified CMR model (MCMR) was used:

$$\tau = \tau_m (1-\exp\{-\beta s/s_m\})^{\alpha} \qquad (7)$$

For each bar type, the constants were evaluated (by minimizing the difference between measured and predicted bond stress – least squares fit) and are reported in Table 6. It should be noted that the proposed empirical formulas are limited to the ranges of pressures tested, and that each bar type will typically have different coefficients. These formulas may be useful for calibration of simple numerical models that can compute the bond stress-slip response as a function of radial normal stress, σ. The models are often applied via interface, or nodal-tie elements. Unfortunately, their application is not as straight forward as their simple form would suggest. The main problem is defining σ. The bond experiments in this study were designed to provide a measure of the average normal component of the interface traction. In most situations, σ is a result, in part, of the mechanical interlocking and as such σ is not known a priori. The approach taken in Part II of this study is to further develop and calibrate a different and more complete bond model that incorporates both σ and the interface dilation (representing the radial deformation produced by the mechanical interlocking within the context of an interface idealization). With this type of formulation, the bond model actively determines σ, and thus can potentially predict both pull-out and splitting failures.

CONCLUSIONS

Bond properties for four types of FRP rebar with different deformation patterns were analyzed experimentally in lightweight concrete. Local bond stress-slip and bond stress-radial displacement responses were obtained for various levels of axisymmetric radial confining pressure. These responses can be considered configuration independent and can be used to develop more general bond models. It was also found that:

1) Surface deformations with a height at least 6% of the nominal rebar diameter (i.e. similar to that of steel) and deformation spacing of not more than 3 times the rebar diameter, were sufficient to yield maximum bond stresses up to 8 MPa (1160 psi) or more, about twice the concrete tensile strength (Types A and D bars). Bars with small surface deformation height of 0.3% of the nominal diameter squeezed through the concrete (Type B). Bars with deformation spacing about 15 times the bar diameter twisted and squeezed through the concrete (Type C).
2) For bars with adequate height and deformation spacing (Types A and D), bond strength could be increased more than twofold by increasing the confining pressure.
3) Estimated development lengths were obtained for various CFRP rebars.
4) Equation (2) (ACI 440, 2001) appears to conservatively predict development values. However, it does not take into consideration the specific shape of the bar deformations,

neither does it set a minimum deformation standard for its usage – this could potentially yield unconservative results for bars with small deformations.

5) Experimental parameters for simple analytical models were obtained, to ease the use of the experimental data.

ACKNOWLEDGMENT

Funding for the present study was provided by the Office of Naval Research, under Mr. Jim Kelly and Dr. Ignacio Perez. Testing support provided by Mr. John Crahan and Mr. Robert Jamond is gratefully acknowledged. CFRP bar samples were provided by Marshall Industries Composites Inc., Prof. Charles W. Dolan, University of Wyoming, and Prof. Srinivasa L. Iyer, South Dakota School of Mines and Technology. The second author was supported, during the writing of this paper, by an appointment to the Research Participation Program at the U.S. Army Research Laboratory administered by the Oak Ridge Institute for Science and Education through an interagency agreement between the U.S. Department of Energy and USARL.

REFERENCES

Achillides, Z., Pilakoutas, K., Waldron P. (1997), "Bond Behaviour of FRP Bars to Concrete," FRPRCS-3, Non-metallic (FRP) reinforcement for concrete structures, Third FRP International Symposium, Japan Concrete Institute, Sapporo, Japan, Vol. 2, pp. 341-348.

ACI 318 (1999), "Building Code Requirements for Structural Concrete," American Concrete Institute, P.O. Box 9094, Farmington Hills, MI 48333.

ACI 440 Committee on Fiber Reinforced Polymer Reinforcement (2001), "Guide for the Design and Construction of Concrete Reinforced with FRP Bars," ACI 440.1R-01, American Concrete Institute, P.O. Box 9094, Farmington Hills, MI 48333.

ASCE Task Committee on Finite Element Analysis of Reinforced Concrete Structures (1982), State-of-the-Art Report on Finite Element Analysis of Reinforced Concrete, American Society of Civil Engineers, 1982, 545 pp.

ASTM D 3916 (1984), "Test Method for Tensile Properties of Pultruded Glass-Fiber-Reinforced Plastic Rod," Annual Book of ASTM Standards, V. 08.03.

Bakht, B., Al-Bazi, G., Banthia, N., Cheung, M., Erki, M.A., Faoro, M., Machida, A., Mufti, A.A., Neale, K., Tadros, G. (2000), "Canadian Bridge Design Code Provisions for Fiber-Reinforced Structures," Journal of Composites for Construction, Vol. 4, No. 1, pp. 3-15.

Benmokrane, B., Chennouf, A. (1997), "Pull-out Behavior of FRP Ground Anchors," 42nd SAMPE Symposium and Exhibition, Anaheim, CA, Vol. 42, No. 1, pp. 311-324.

Benmokrane, B., Rahman, H., editors (1998), First International Conference on Durability of Composites for Construction, CDCC'98, Sherbrooke (Québec), Canada.

Ciampi, V., Eligehausen R., Bertero V.V., Popov E.P. (1981), "Analytical model for Deformed Bar Bond under Generalized Excitations," IABSE Colloquium on Advanced Mechanics in Reinforced Concrete, Delft, The Netherlands.

Cosenza, E., Manfredi, G., Realfonzo, R. (1995), "Analytical Modeling of Bond Between FRP Reinforcing Bars and Concrete," FRPRCS-2, Non-Metallic (FRP) Reinforcement for Concrete Structures, Second FRP International Symposium, Gent, pp. 165-171.

Cosenza, E., Manfredi, G., Realfonzo, R. (1997), "Behavior and Modeling of Bond of FRP Rebars to Concrete," Journal of Composites for Construction, Vol. 1, No. 2, pp. 40-51.

Cosenza, E., Manfredi, G., Pecce, M., Realfonzo, R. (1999), "Bond between Glass Fiber Reinforced Plastic Reinforcing Bars and Concrete – Experimental Analysis," FRPRCS-4, Fourth Intl. Symposium on Fiber Reinforced Polymer Reinforcement for Reinforced Concrete Structures, ACI SP-188, Baltimore, MD, pp. 347-358.

Cox, J.V. (1994), "Development of a Plasticity Bond Model for Reinforced Concrete - Theory and Validation for Monotonic Applications," PhD Thesis, University of California, Davis.

Cox, J.V. (1998), "A Dilatational Interface Model for Bond," Bond and Development of Reinforcement, ACI SP-180, American Concrete Institute, pp. 81-103.

Cox, J.V., Bergeron, K., Malvar, L.J. (2000), "A Combined Experimental and Numerical Study of the Bond between Lightweight Concrete and CFRP Bars," Sessions on Interface Degradation, 14th ASCE Engineering Mechanics Conference, The University of Texas at Austin.

Cox, J.V., Guo, J. (1999), "Modeling Stress State Dependency of Bond Behavior of Fiber Reinforced Polymer Tendons," FRPRCS-4, Fourth International Symposium on Fiber Reinforced Polymer Reinforcement for Reinforced Concrete Structures, ACI SP-188, Baltimore, MD, pp.791-805.

Cox, J.V., Herrmann, L.R. (1992), "Confinement Stress Dependent Bond Behavior, Part II: A Two Degree of Freedom Plasticity Model," Bond in Concrete, Proceedings of the International Conference, Riga, Latvia, pp. 11/11-11/20.

Cox, J.V., Herrmann, L.R. (1998), "Development of a Plasticity Bond Model for Steel Reinforcement," Mechanics of Cohesive-Frictional Materials, vol 3, 1998, pp. 155-180.

Cox, J.V., Herrmann, L.R. (1999), "Validation of a Plasticity Bond Model for Steel Reinforcement," Mechanics of Cohesive-Frictional Materials, vol 4, 1999, pp. 361-389.

Dolan, C.W., Rizkalla, S.H., Nanni, A., editors, (1999), Fourth International Symposium on Fiber Reinforced Polymer Reinforcement for Reinforced Concrete Structures, FRPRCS-4, ACI SP-188, Baltimore, MD.

Eligehausen, R., Popov, E.P., Bertero, V.V. (1983), "Local Bond Stress-Slip Relationships of Deformed Bars under Generalized Excitations," Report No. UCB/EERC 83/23, Earthquake Engineering Research Center, University of California, Berkeley.

FIB Bulletin 10 (2000), “Bond of Reinforcement in Concrete,” State-of-the-art Report, Fédération Internationale du Béton, Federal Institute of Technology, Département Génie Civil, Lausanne, Switzerland.

Focacci, F., Nanni, A., Bakis, C.E. (2000), “Local Bond-Slip Relationship for FRP Reinforcement in Concrete,” Journal of Composites for Construction, Vol. 4, No. 1, pp. 24-31.

Gambarova, P.G., Rosati, G.P., Schumm, C.E. (1998), “Bond and Splitting: A Vexing Question,” Bond and Development of Reinforcement, ACI SP-180, American Concrete Institute, pp. 23-43.

Iyer, S.L., Sivakumar, R. (1994), "Graphite Prestressed Piles and Fiberglass Prestressed Pilecaps for U.S. Navy Pier in California,” Infrastructure: New Materials and Methods for Repair, 3rd Materials Engineering Conference (K. Basham, ed.), San Diego, CA, pp. 392-399.

Keuser, M., Mehlhorn, G. (1987), "Finite Element Models for Bond Problems," Journal of Structural Engineering, ASCE, V. 113, No. 10, pp. 2160-2173.

Lundgren, K., Magnusson, J. (2001), “Three Dimensional Modeling of Anchorage Zones in Reinforced Concrete,” Journal of Engineering Mechanics, Vol. 127, No. 7, pp. 693-699.

Lundgren, K., Gylltoft, K. (2000), “A Model for the Bond between Concrete and Reinforcement,” Magazine of Concrete Research, Vol. 52, No. 1, pp. 53-63.

Mahmoud, Z.I., Rizkalla, S.H., Zaghloul, E.R. (1999), “Transfer and Development Lengths of Carbon Fiber Reinforced Polymers Prestressing Reinforcement,” ACI Structural Journal, Vol. 96, No. 4, pp. 594-602.

Malvar, L.J. (1992a), "Confinement Stress Dependent Bond Behavior, Part I: Experimental Investigation," Bond in Concrete, Proceedings of the International Conference, Riga, Latvia, pp. 1/79-1/88.

Malvar, L.J. (1992b), "Bond of Reinforcement under Controlled Confinement," ACI Materials Journal, V. 89, No.6, November-December 1992, pp. 593-601.

Malvar, L.J. (1992c), "Bond of Reinforcement under Controlled Radial Pressure," Studi e Ricerche, V. 13-1992, Structural Engineering Department, Polytechnic University of Milan, Milan, Italy, pp. 83-118.

Malvar, L.J. (1995), "Tensile and Bond Properties of GFRP Reinforcing Bars," ACI Materials Journal, vol. 92, no. 3, pp. 276-285.

Malvar, L.J. (1998), “Durability of Composites in Concrete,” First International Conference on Durability of Composites for Construction, CDCC’98, Sherbrooke, Canada, pp. 361-372.

McCabe, S.L., Pantazopoulou, S.J. (1998), “Evaluation of Bond Performance in Reinforced Concrete Structures,” Bond and Development of Reinforcement, ACI SP-180, American Concrete Institute, pp. 1-21.

Nanni, A., Conrad, J.O., Bakis, C.E., Uchno, J. (1997), “Material Properties of C-Bar Reinforcing Bar,” Civil Engineering Department, Pennsylvania State University, PA (also Research Bulletin 97-005, Marshall Industries Composites, Lima, OH).

Razaqpur, A.G., editor (2000), Third International Conference on Advanced Composite Materials in Bridges and Structures, ACMBS-3, Ottawa, Canada, August 2000.

Rizkalla, S., Abdelrahman, McVey, M. (1997), "Material Properties of C-Bar Reinforcing Rod," ISIS Canada, Winnipeg, Manitoba, Canada (also Research Bulletin 97-006, Marshall Industries Composites, Lima, OH).

Saadatmanesh, H., Ehsani, M.R., editors (1998), Fiber Composites in Infrastructure, Second Intl. Conference on Composites in Infrastructure, ICCI'98, Tucson, AZ.

Shield, C.K., French, C.W., Hanus, J.P. (1999), "Bond of Glass Fiber Reinforced Plastic Reinforcing Bar for Consideration in Bridge Decks," FRPRCS-4, Fourth International Symposium on Fiber Reinforced Polymer Reinforcement for Reinforced Concrete Structures, ACI SP-188, Baltimore, MD, pp. 393-406.

Sonobe, Y., Fukuyama, H., Okamoto, T., Kani, N., Kimura, K., Kobayashi, K., Masuda, Y., Matsuzaki, Y., Mochizuki, S., Nagasaka, T., Shimizu, A., Tanano, H., Tanigaki, M., Teshigawara, M. (1997), "Design Guidelines of FRP Reinforced Concrete Building Structures," Journal of Composites for Construction, pp. 90-115.

Taly, N., GangaRao, H.V.S. (2001), "Bond Behavior of FRP Reinforcing Bars – The State of the Art," 46th International SAMPE Symposium, Long Beach, Vol. 2, pp. 1784-1796.

Tepfers, R., Molander, I., Thalenius, K. (1992), "Experience from Testing of Concrete Reinforced with Carbon Fiber and Aramid Fiber Strands," XIV Nordic Concrete Congress and Nordic Concrete Industry Meeting, pp. 337-347 (also in Publication 92:6, Chalmers Institute of Technology, Göteborg, Sweden).

Tokyo Rope Manufacturing Co. Ltd. (1989), "CFCC Technical Data", Corporate Report.

Tork, B.S. (1999), "Study of the Combined Mechanisms of Fissuration and Bond in Reinforced and Prestressed Concrete Members," Ph.D. Thesis, Escuela Technica Superior de Ingenieros de Caminos Canales y Puertos, Polytechnic University of Madrid, Spain (in Spanish).

Unified Facilities Guide Specifications (1999), "Marine Concrete," UFGS 03311, Joint Departments of the Army, Air Force and Navy, Washington, D.C.

Yamaguchi, T., Kato, Y., Nishimura, T., Uomoto, T. (1997), "Creep Rupture of FRP Rods Made of Aramid, Carbon and Glass Fibers," FRPRCS-3, Third International Symposium on Non-Metallic (FRP) Reinforcements for Concrete Structures, Japan Concrete Institute, Sapporo, Japan, Vol. 2, pp. 179-186.

TABLE 1. BAR DATA.

TYPE	**A**	**B**	**C**	**D**
Resin	Epoxy/Vinyl.	Epoxy	Vinylester	Epoxy
Fiber Volume, %	60	65	65	64
Surface pattern	ribs like steel bar	textured	7-strand cable	7-strand cable
Bar Diameter, mm (in)	10.2 (0.4)	8.2 (0.32)	10.6 (0.42)	9.8 (0.39)
Bar Area, mm^2 (in^2)	81.1 (0.126)	52.8 (0.082)	87.9 (0.136)	76.0 (0.118)
Deformation Spacing mm (in)	7.6 (0.3)	3.0 (0.12)	150 + (6 +)	30 (1.2)
Deformation Height mm (in)	0.6 (0.024)	0.025 (0.001)	1.4 (0.055)	1.1 (0.043)
Ultimate Stress MPa (ksi)	1586 (230)	1456 (211)	1931 (280)	1871 (271)
Elastic Modulus GPa (ksi)	113 (16,400)	139 (20,200)	157 (22,800)	137 (19,900)

TABLE 2 – PREVIOUS TEST RESULTS

BAR TYPE	REFERENCE	BAR DIAMETER mm (in)	BAR STIFFNESS GPa (ksi)	BAR STRENGTH MPa (ksi)	CONCRETE STRENGTH MPa (psi)	SPECIMEN SIZE LxD or LxWxD mm (in)	BOND STRENGTH MPa (psi)	BOND LENGTH bar diameters
A (GFRP)	Cosenza et al. (1999)	12.7 (0.5)	42 (6,090)	770 (112)	39 (5,655)	127x150x150 (5x6x6)	14.5 (2,100)	10*
A (GFRP)	Shield et al. (1999)	15.9 (0.625)	42 (6,090)	427 (61.9)	29.7 (4,300)	381x305x457 (15x12x18)	4.5 (650)	24*
A (GFRP)	Nanni et al. (1997)	13 (0.5)	37.5 (5,437)	568 (82.4)	34.5 (5,000)	150x150x150 (6x6x6)	17 (2,465)	2.5 and 5
A (GFRP)	Rizkalla et al. (1997)	12 (0.5)	40.6 (5,890)	640 (92)	44 (6,380)	-	21.3 (3,090)	15*
C	Iyer et al. (1994)	12.7 (0.5)	-	1,860 (270)	-	-	-	-
D	Benmokrane et al. (1997)	7.3 (0.29)	140 (20,249)	2,218 (322)	61.6 (8,930)	150x57 (6x2.2)	6.21 (901)	13.7
D	Tepfers et al. (1992)	12.5 (0.5)	137 (19,865)	1,765 (256)	47.3 (6,860)	48x115 (1.9x4.5)	9.5 (1,338)	3.8
D	Tepfers et al. (1992)	12.5 (0.5)	137 (19,865)	1,765 (256)	44.4 (6,440)	200x200x200 (8x8x8)	13 (1,885)	3.6
D	Tokyo Rope (1989)	12.5 (0.5)	137 (19,865)	1,158 (168)	47.6 (6,900)	150x100x100 (6x4x4)	7.23 (1,048)	12
any	Sonobe et al. (1997)	-	-	-	-	100x100x100 (4x4x4)	-	23*

* development length

TABLE 3 – CONCRETE PROPERTIES

CONCRETE PROPERTIES	**BOND TESTS**				**LONG EMBEDMENT TESTS**
Bar Type	A	B	C	D	A, B, C, D
Tensile Strength f_t MPa (psi)	3.72 (540)	3.85 (558)	3.78 (548)	3.72 (540)	4.53 (657)
Compressive Strength f_c, MPa (psi)	34.43 (4993)	50.97 (7390)	39.35 (5706)	34.43 (4993)	42.94 (6228)
Modulus of Elasticity E GPa (ksi)	12.77 (1852)	15.65 (2269)	12.54 (1818)	12.77 (1852)	17.03 (2469)

TABLE 4 – PEAK BOND STRESS AND CORRESPONDING SLIP

BAR TYPE	CONFINEMENT MPa	CONFINEMENT psi	PEAK BOND STRESS MPa	PEAK BOND STRESS psi	PEAK BOND STRESS x f_t	SLIP mm	SLIP in
A	3.45	500	4.23	613	1.14	0.292	0.0115
	10.3	1500	6.26	908	1.68	0.632	0.0249
	17.2	2500	8.10	1175	2.18	0.863	0.0340
	24.1	3500	10.10	1465	2.71	1.056	0.0115
B	3.45	500	2.23	323	0.58	0.133	0.0052
	10.3	1500	4.26	618	1.11	0.777	0.0306
	17.2	2500	3.76	545	0.98	0.732	0.0285
	24.1	3500	3.59	521	0.93	1.124	0.0443
C	3.45	500	3.36	487	0.89	0.645	0.0254
	10.3	1500	3.94	571	1.04	8.044	0.3167
	17.2	2500	4.72	684	1.25	9.795	0.3856
	24.1	3500	5.95	863	1.57	7.961	0.3134
D	3.45	500	5.10	740	1.37	0.199	0.0078
	10.3	1500	5.98	867	1.61	0.332	0.0131
	17.2	2500	7.93	1150	2.13	0.317	0.0125
	24.1	3500	8.27	1199	2.22	0.291	0.0115

TABLE 5 – LONG EMBEDMENT TESTS RESULTS

BAR TYPE	TEST	FAILURE LOAD kN (kips)	BAR STRESS AT FAILURE MPa (ksi)	FAILURE MODE
A	1	64.8 (14.6)	798 (115.6)	Bar slipped once inside cylinder at maximum load Cylinder split into 3 segments after reloading
A	2	101.5 (22.8)	1250 (181.2)	Bar slipped at maximum load 3 times Cylinder split into 3 segments after reloading
B	1	63.8 (14.4)	1207 (175.1)	Bar slipped twice, broke near concrete
B	2	66.0 (14.8)	1248 (181.0)	Bar slipped at maximum load twice, pulled out
C	1	116.4 (26.2)	1327 (192.4)	Bar slipped 3 times, cylinder split after reloading
C	2	119.0 (26.8)	1357 (196.8)	Bar slipped twice, cylinder split after reloading
D	1	45.6 (10.3)	600 (86.9)	Cylinder split into 3 segments at first loading
D	2	135 (30.4)	1776 (257)	Cylinder split at first loading, bar pulled out

TABLE 6 - ANALYTICAL FIT PARAMETERS

BAR	PARAMETER						
	A	B	C	D	BEP α	MCMR α	MCMR β
Type A	0.881	0.282	0.0202	0.0134	0.30	1.0	4.6
Type B	0.713	0.052	0.0129	0.0199	0.13	0.2	2.0
Type C	0.736	0.124	0.1766	0.1225	0.11	0.2	3.0
Type D	1.215	0.167	0.0232	0.0013	0.30	1.0	4.6

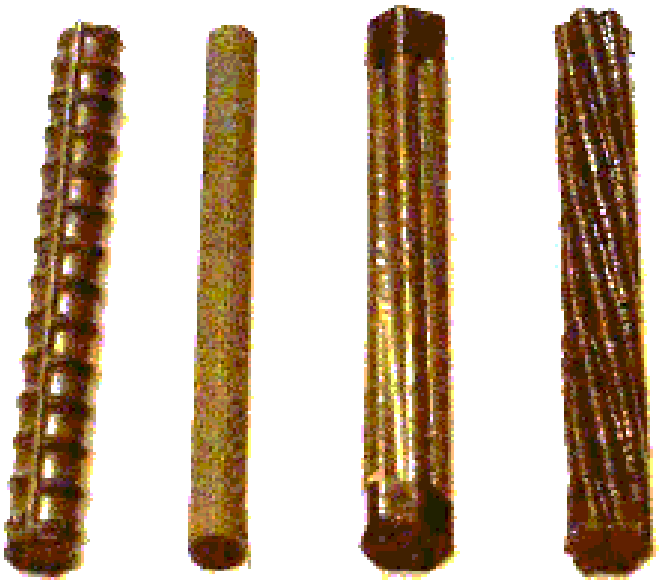

Figure 1. CFRP bar types

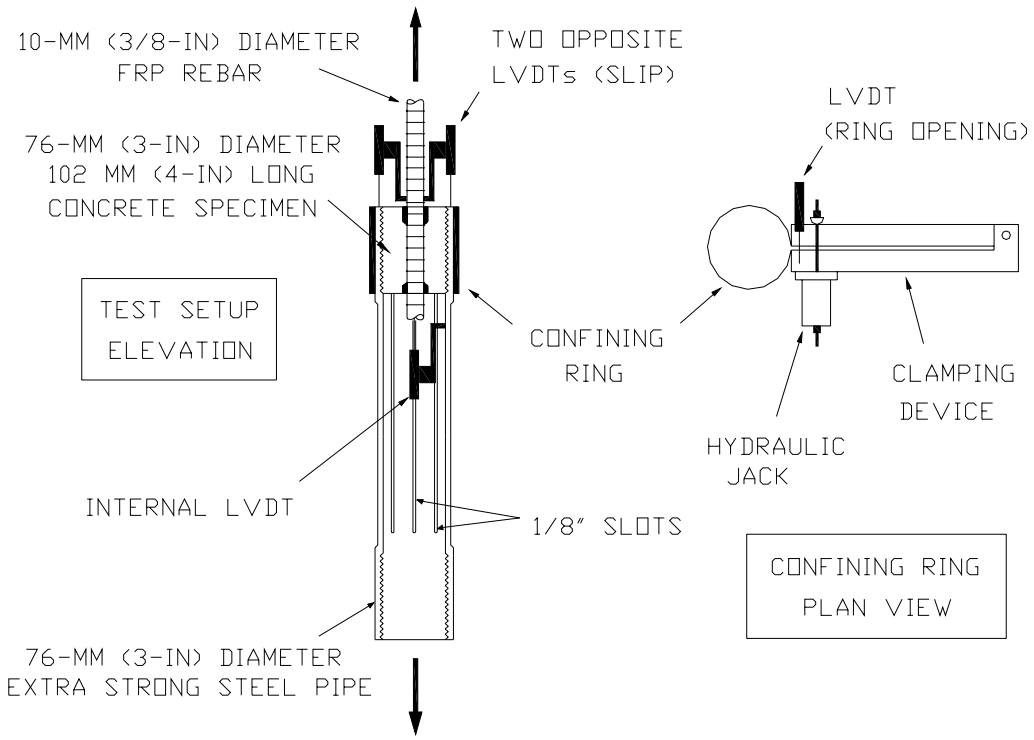

Figure 2. Test set up schematic

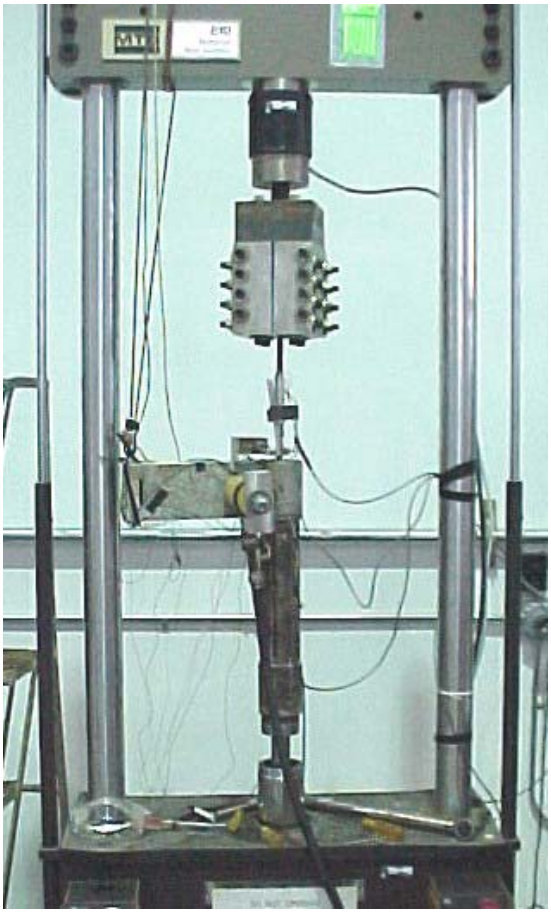

Figure 3. Test set up

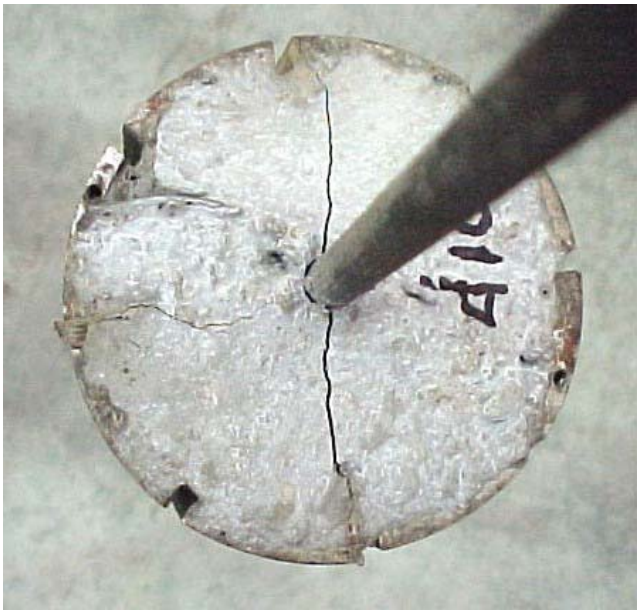

Figure 4. Tested specimen

Figure 5. Long embedment test specimen

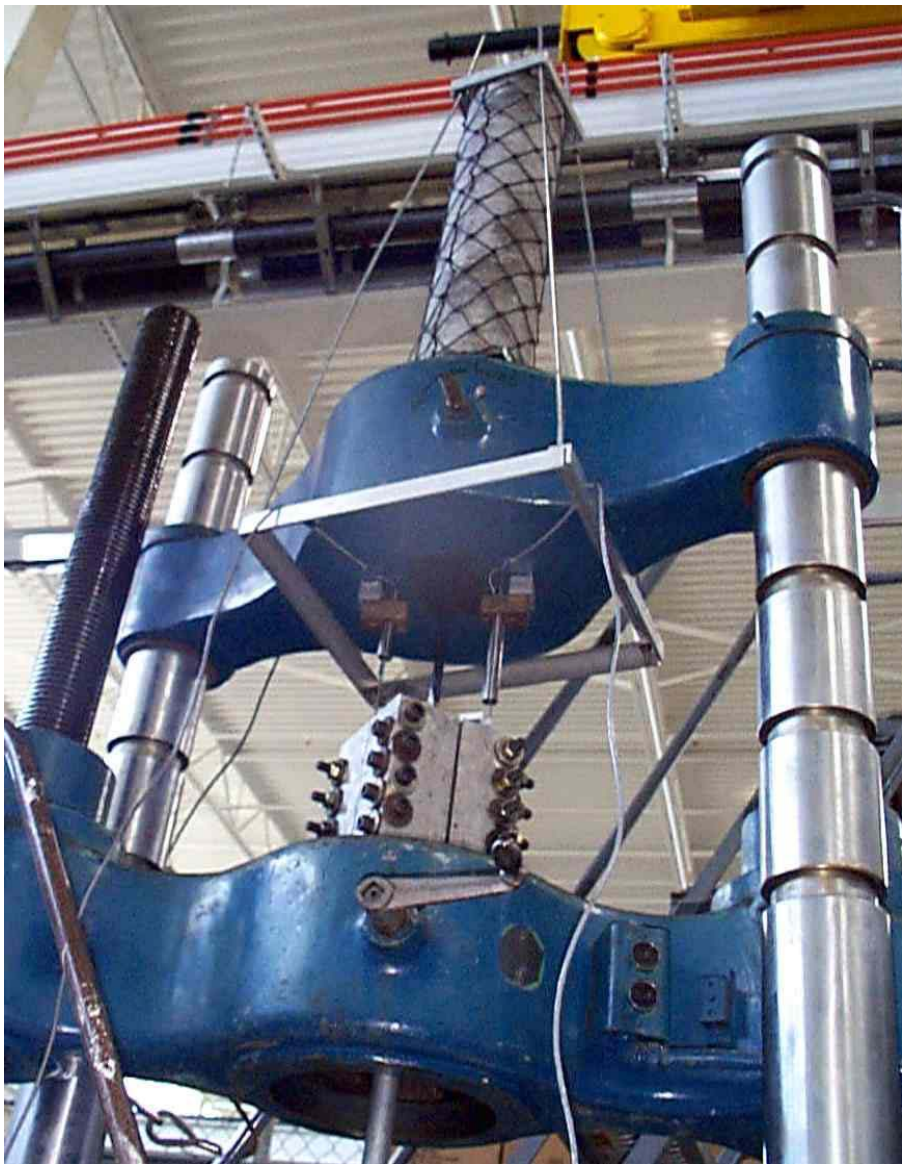

Figure 6. Testing of long test specimen

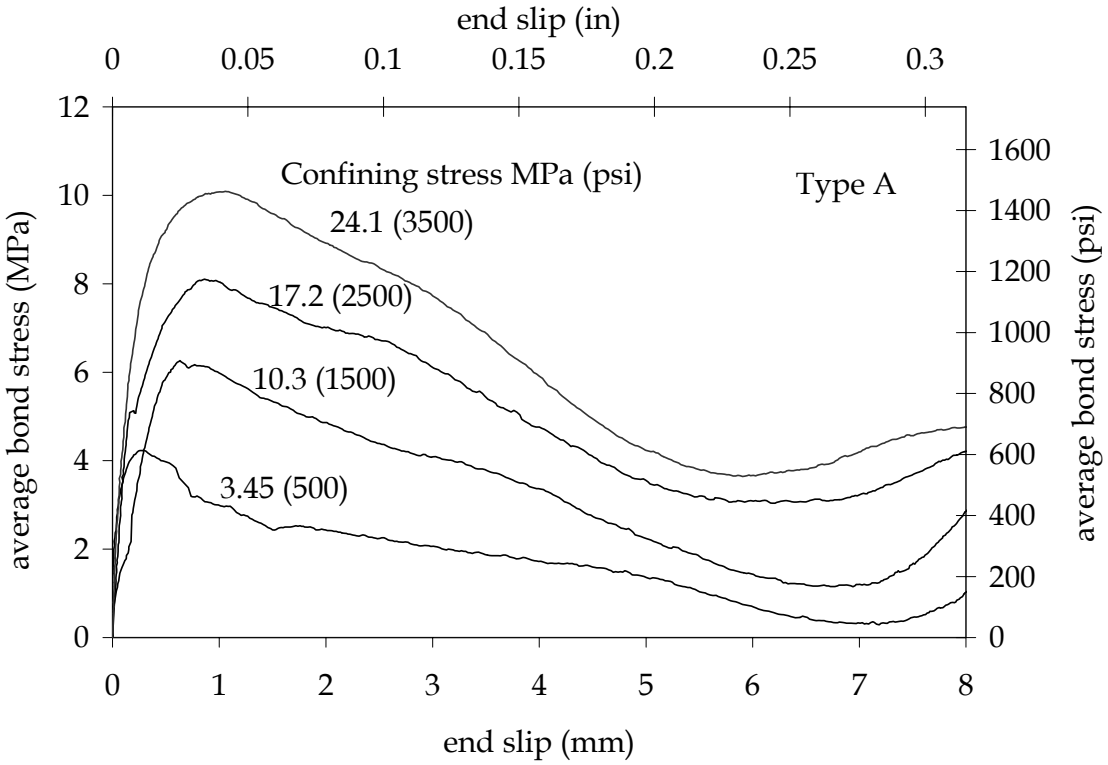

Figure 7. Bond stress versus slip for Type A bar.

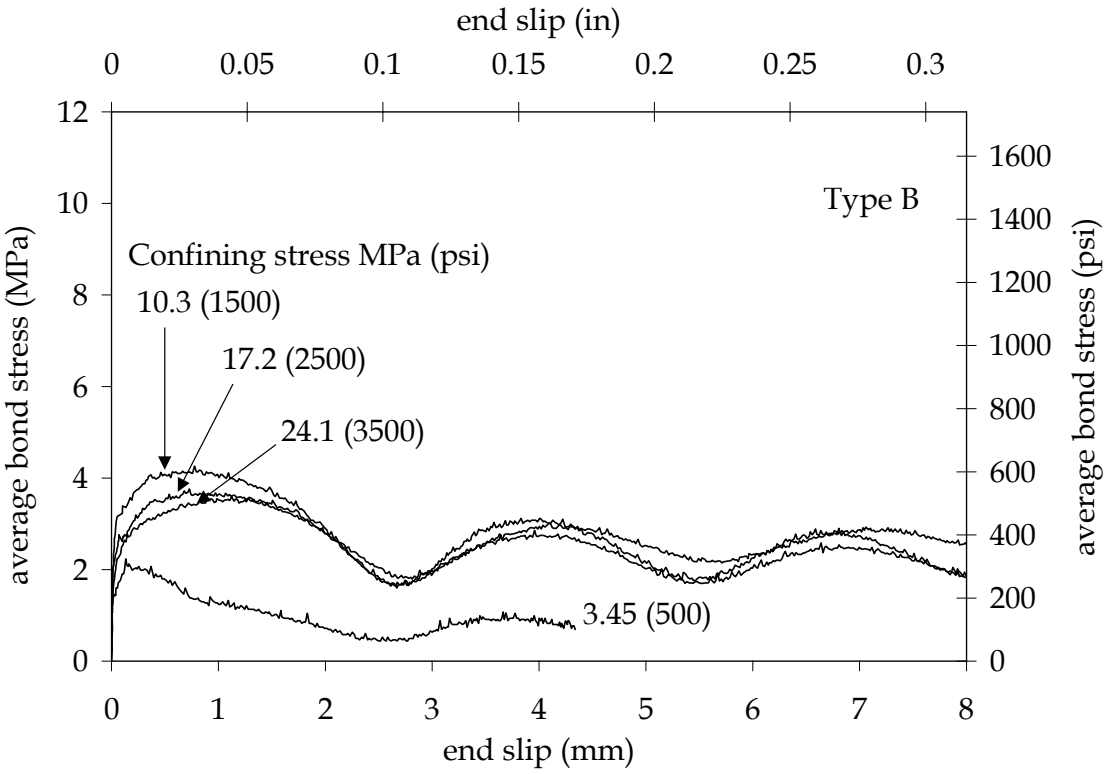

Figure 8. Bond stress versus slip for Type B bar.

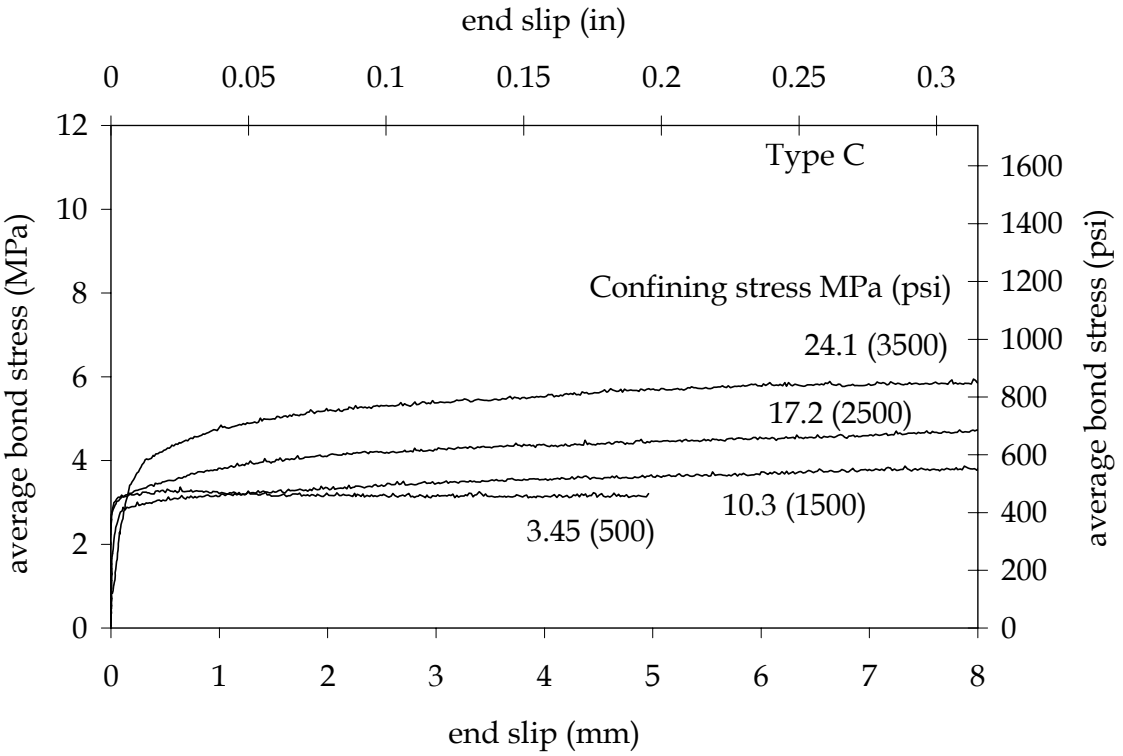

Figure 9. Bond stress versus slip for Type C bar.

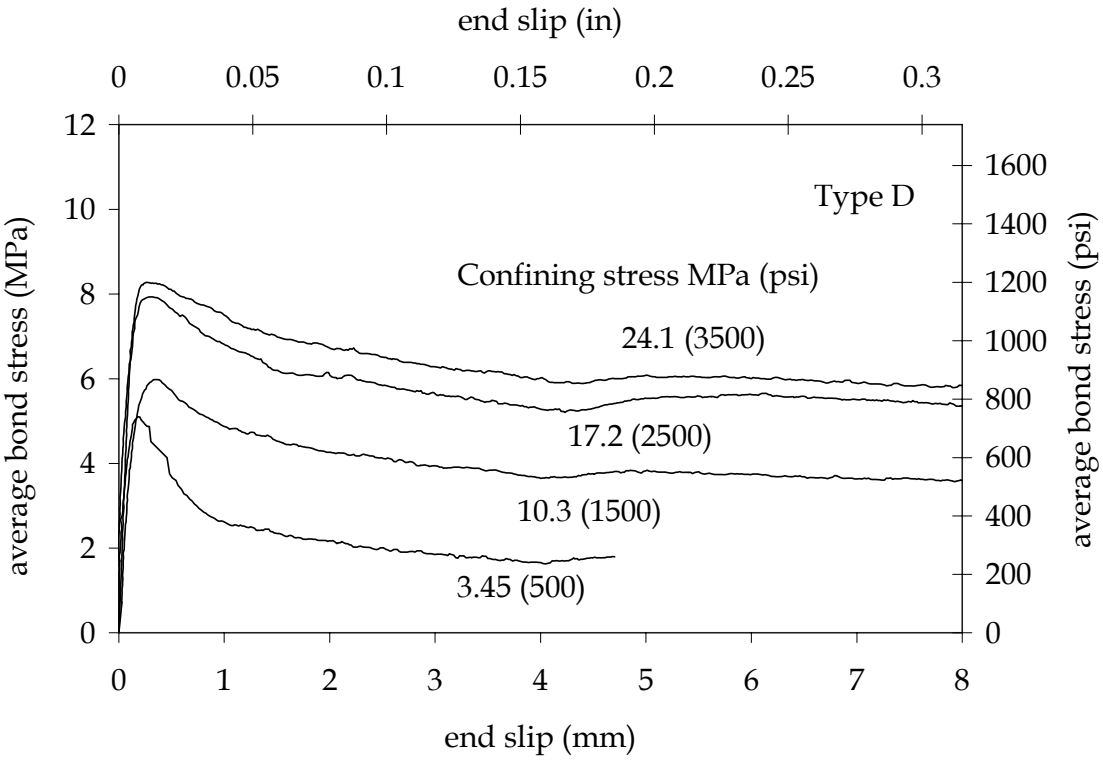

Figure 10. Bond stress versus slip for Type D bar.

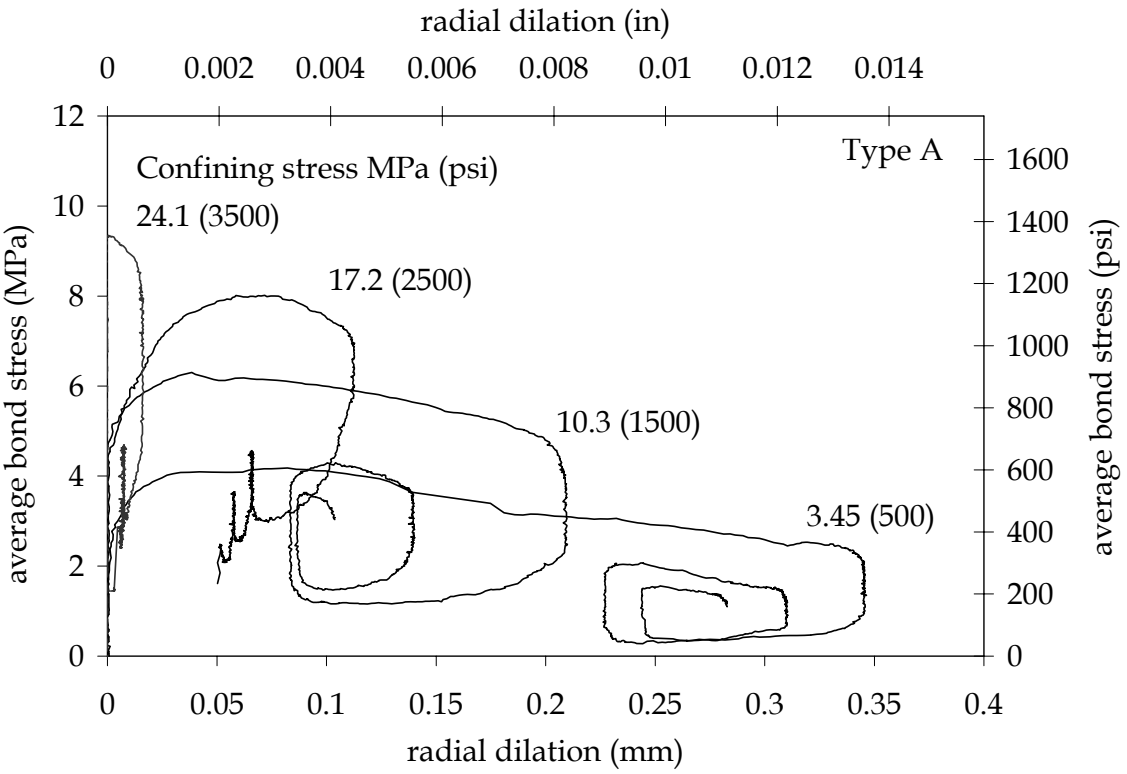

Figure 11. Bond stress versus radial dilation for Type A bar.

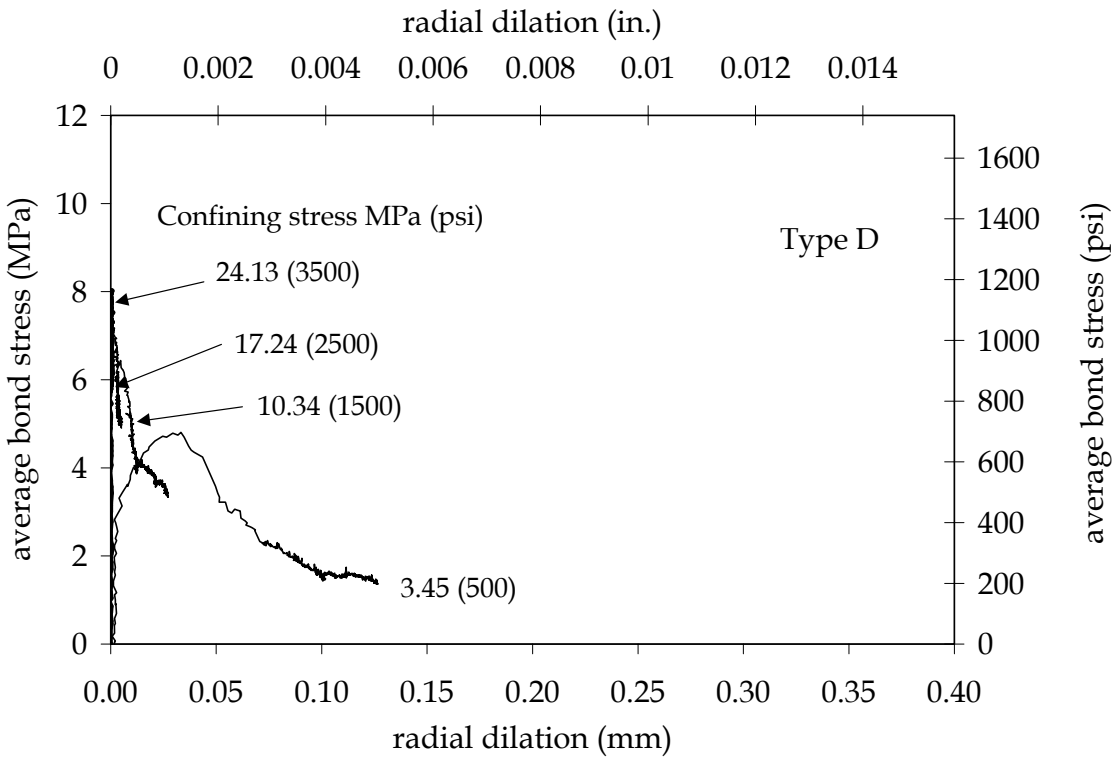

Figure 12. Bond stress versus radial dilation for Type D bar.

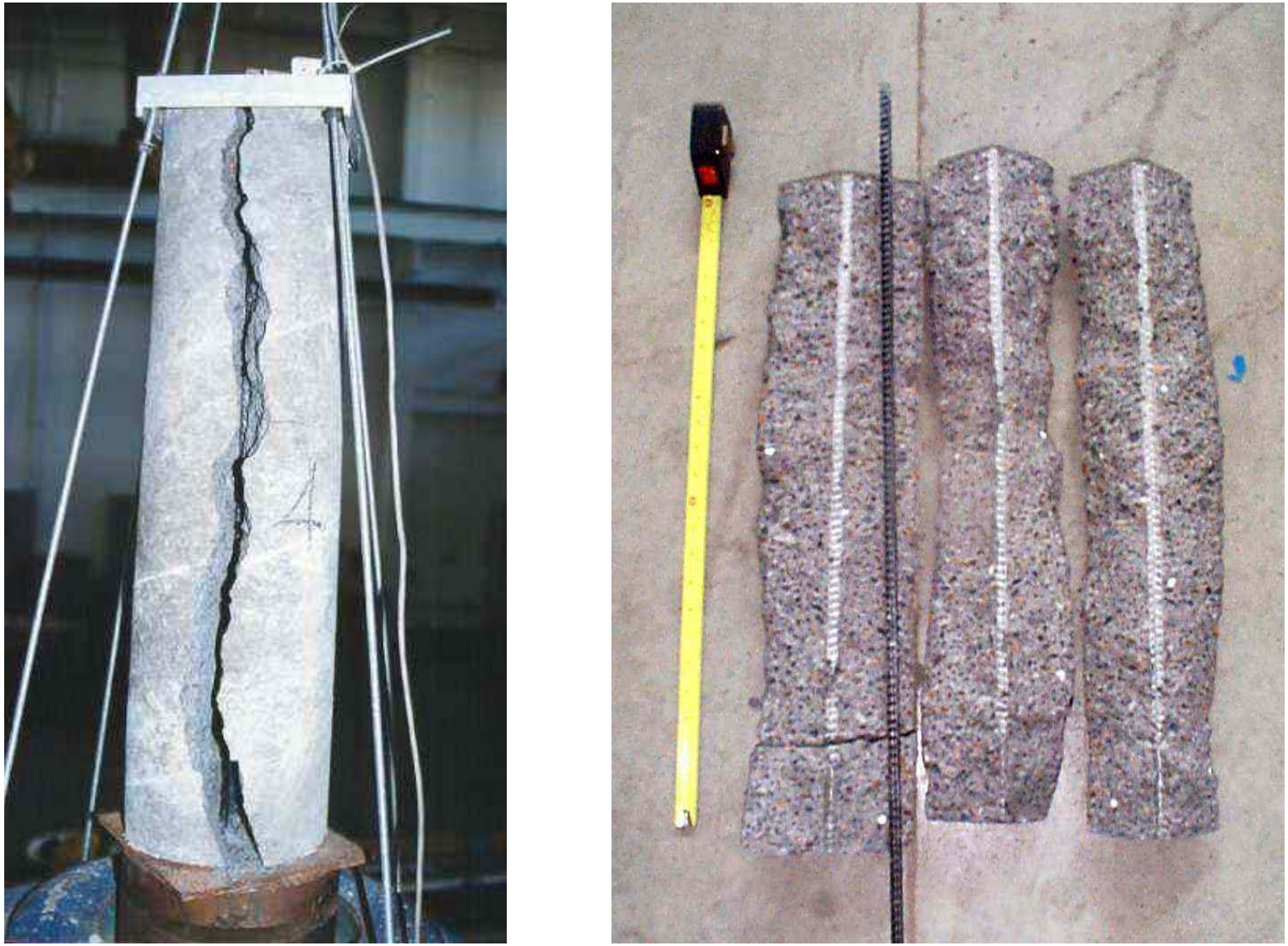

Figure 13. Splitting of long embedment test specimens.